

## **$\mu$ -Opioid Receptor Cell Surface Expression Is Regulated by Its Direct Interaction with RibophorinI**

Xin Ge<sup>†\*</sup>, Horace H. Loh<sup>†</sup> and Ping-Yee Law<sup>†</sup>.

Department of Pharmacology, University of Minnesota Medical School,  
Minneapolis, MN 55455, USA

Running title: *RPNI Enhances MOR Cell Surface Expression*

Corresponding author: Xin Ge

Department of Pharmacology  
University of Minnesota Medical School  
6-120 Jackson Hall, 321 Church St. SE  
Minneapolis, MN 55455, USA  
TEL: 612-626-6539  
FAX: 612-625-8408  
E-Mail: [gexx0019@umn.edu](mailto:gexx0019@umn.edu)

Number of text pages: 36

Number of tables: 1

Number of figures: 7

Number of references: 38

Number of words in abstract: 153

Number of words in introduction: 414

Number of words in discussion: 1330

*Abbreviations:* GPCR, G protein-coupled receptor; MOR,  $\mu$ -opioid receptor; DOR,  $\delta$ -opioid receptor; KOR,  $\kappa$ -opioid receptor; RPNI, ribophorin I; N2A, neuro2A neuroblastoma cell; ER, endoplasmic reticulum; DMEM, Dulbecco's modified Eagle's medium; G418, Geneticin; IP, Immunoprecipitation; IB, Immunoblot; MALDI-TOF, Matrix Assisted Laser Desorption /Ionization- Time Of Flight mass spectrometry; LC-MS/MS, Liquid chromatography-electrospray ionization tandem mass spectrometry; PBS, Phosphate-buffered saline; FACScan, fluorescence flow cytometry; PA, Ponasterone A; OST, Oligosaccharide transferase; MOR5ND, MOR with Asn<sup>9</sup>, Asn<sup>31</sup>, Asn<sup>38</sup>. Asn<sup>46</sup> and Asn<sup>53</sup> residues at the N-terminus all mutated to Asp; C2, MOR with the <sup>344</sup>KFCTR<sup>348</sup> sequence delete.

## Abstract

The trafficking of the  $\mu$ -opioid receptor (MOR), a member of rhodopsin GPCR family, can be regulated by interaction with multiple cellular proteins. In order to determine the proteins involved in receptor trafficking, using the targeted proteomic approach and mass spectrometry analysis, we have identified that Ribophorin I (RPNI), a component of the oligosaccharidetransferase complex, could directly interact with MOR. RPNI can be shown to participate in MOR export by the intracellular retention of the receptor after siRNA knocking-down of endogenous RPNI. Over-expression of RPNI rescued the surface expression of the MOR<sup>344</sup>KFCTR<sup>348</sup> deletion mutant (C2) independent of calnexin. Furthermore, RPNI regulation of MOR trafficking is dependent on the glycosylation state of the receptor, as reflected by the inability of over-expression of RPNI to affect the trafficking of the N-glycosylation deficient mutants, or GPCRs that have minimal glycosylation sites. Hence, this novel RPNI chaperone activity is a consequence of N-glycosylation-dependent direct interaction with MOR.

## Introduction

Being a member of the GPCR superfamily and rhodopsin subfamily, opioid receptors ( $\mu$ ,  $\delta$ ,  $\kappa$ ) have the putative structures of seven transmembrane domains and an extracellular N terminus with multiple glycosylation sites (Evans *et al.*, 1992; Kieffer *et al.*, 1992; Chen *et al.*, 1993). When synthesis occurs, the completed core oligosaccharide is transferred from the dolichylpyrophosphate carrier to a growing, newly synthesized polypeptide chain, which is coupled through an N-glycosidic bond to the side chain of an asparagine residue. The oligosaccharyltransferase responsible for this transfer is a complex enzyme with its active site in the ER lumen (Silberstein and Gilmore, 1996). During the translocation into the ER lumen, polypeptides on membrane-bound polysomes may be cotranslationally modified by N-glycosylation (Kreibich *et al.*, 1983). In this process, the OST catalyzes the transfer of high mannose oligosaccharides, which are preassembled on lipid-anchored dolicholpyro-phosphate moieties to an asparagine residue within an Asn-X-Ser/Thr consensus motif of nascent polypeptide chains facing the lumen of the ER (Abeijon and Hirschberg, 1992). Immediately after coupling to the polypeptide chain, terminal glucose and mannose residues are removed by ER glucosidases and mannosidases (Kornfeld and Kornfeld, 1985). When the glycoprotein moves to the Golgi complex, the glycan chains undergo further trimming of mannoses. N-glycosylation has been found to be an important factor in the regulation of protein folding, stability, sorting and secretion (Helenius and Aebi, 2001). For opioid receptors, this N-glycosylation is a rate-limiting step in their translocation to the cell membrane (Petaja-Repo *et al.*, 2000). However, the detailed mechanism of the opioid receptors biosynthesis is still elusive. A truncated form (38-117) of GEC1 was found to specifically interact with the C-tail of the human kappa opioid receptor (hKOR) and be important for trafficking hKOR in the biosynthesis pathway

(Chen et al., 2006). Whether proteins similar to GEC1 participate in MOR maturation process remains unknown.

In order to identify the binding partners of MOR, we purified the MOR complexes from neuroblastoma neuro2A (N2A) cells stably expressing (His)<sub>6</sub>-tagged MOR using the Ni<sup>2+</sup>-resin affinity column chromatography. We found ribophorin I (RPNI), a member of the oligosaccharide transferase family that was assumed to be responsible for N-glycosylation of newly synthesized proteins, could interact with MOR specifically. Furthermore, our results showed that RPNI was a critical mediator of the MOR transport from the endoplasmic reticulum (ER) to the cell membrane. Our data demonstrate that, in addition to N-glycosylation, RPNI acts as a novel key regulator in the transport of nascent receptors, thus affecting MOR function.

## **Materials and Methods**

### **Expression of (His)<sub>6</sub>-MOR in the N2A Cells**

The rat MOR tagged with the (His)<sub>6</sub>-epitope at N-terminus was subcloned in pCDNAmp vector. N2A cells were cultured in Dulbecco's modified Eagle's medium (DMEM) supplemented with 100 units/ml penicillin, 100 µg/ml streptomycin, and 10% fetal calf serum (DMEM growth medium) in a 10% CO<sub>2</sub> incubator. These N2A cells then were transfected with 10 µg of the (His)<sub>6</sub>-MOR plasmids. The colonies surviving the antibiotic Geneticin (G418) selection (1 mg/ml) were isolated. The cell clone that expressed MOR at the level of 0.8 pmole/mg protein was used in receptor complex purification.

### **Cell Culture and Transient Transfection**

N2A cells were maintained in DMEM containing 10% fetal bovine serum and penicillin/streptomycin. Cells were plated on 100-mm dishes (for

immunoprecipitation studies) or 6-well plates (for flow cytometry studies) at a density of 250,000 cells/ml, and grown to 80% confluency. Transfections were performed using the Superfect transfection reagent (QiaGen, Valencia CA). Transfection medium was replaced with medium containing fresh serum 12-18 hours after transfection, and cells were harvested 24-48 hours later.

### **Purification of Receptor Complex and Mass Spectrometry**

Sixty 150mm dishes of stably expressing (His)<sub>6</sub>-MOR N2A cells and 150mm dishes of control N2A cells were lysed with 1% Triton X-100 at 4°C for 2 hours. Lysate was collected and centrifuged at 10,000x g for 15 minutes at 4°C. Supernatant was collected and purified by Ni<sup>2+</sup> resin columns (Invitrogen Carlsbad, CA). Then the columns were washed ten times with wash buffer and eluted with elution buffer provided by the kit (Invitrogen Carlsbad, CA). Eluates were concentrated with Amicon concentration cells (Amicon Beverly, MA). Protein was separated by SDS-PAGE and silver-stained, and the presence of MOR was identified by Western analysis.

### **Proteolytic Digestion**

Silver-stained gel bands were excised, dried and destained by incubating in 15 mM K<sub>3</sub>Fe(CN)<sub>6</sub> and 50 mM Na<sub>2</sub>S<sub>2</sub>O<sub>3</sub> at 24°C for 15 minutes, and then washed with 100 mM NH<sub>4</sub>HCO<sub>3</sub>. Destained gels were dried and rehydrated in 50 mM NH<sub>4</sub>HCO<sub>3</sub> and 5 mM CaCl<sub>2</sub> solution with 0.01 mg/ml sequence-grade modified porcine trypsin (Promega, Madison, WI) and incubated at 37°C overnight. Trypsinized fragments were collected by sonicating the gel pieces in 50 µl of 25 mM NH<sub>4</sub>HCO<sub>3</sub> and again after adding 50 µl of 50% acetonitrile. The supernatant was collected and sonicated repeatedly in 50 µl of 5% formic acid and again after adding 50 µl of 50% acetonitrile. The supernatant was pooled.

DTT was added to a final concentration of 1 mM, and the sample was dried and frozen at -80°C for MALDI-TOF or LC MS/MS.

### **LC MS/MS Spectrometry**

Prior to LC MS/MS analysis, the sample was reconstituted with load buffer and the entire sample was injected. LC MS/MS methods were as described in (Kappahn et al., 2003). LC MS/MS results were analyzed by ProteinPilot™ Software 2.0, software revision number 50861 (Applied Biosystems Inc, ABI, (Shilov et al., 2007). The search engine uses biological modification invoked through the search effort (i.e., semi- and non-trypsin peptides are included in the search) as the search parameters. Protein Database was NCBI's nr mouse subset database from musculus\_NCBIInr\_CTM\_20061212, and was appended to a contaminants database (107,806 proteins total).

### **Immunoprecipitation and Western-blot Analysis**

Confluent cells were washed in phosphate-buffered saline (PBS) at 4°C and lysed for 30 minutes in solubilization buffer (1% Triton X-100, 150 mM NaCl, 1 mM EGTA, pH 7.4) containing mammalian protease inhibitor cocktail (Sigma-Aldrich, St. Louis, MO), at 4°C. Lysate was centrifuged for 30 minutes at 10,000 x g, and the supernatant was collected and assayed for protein by the BCA method (Pierce, Rockford, IL). A total of 500 µg of protein was pre-cleared with Protein G Sepharose beads (Sigma-Aldrich) and incubated with 1 µg mouse anti-HA antibodies for 2-3 hours followed by incubation with 30 µl Protein G Sepharose for 3 hours, all at 4°C. Sepharose beads were pelleted by brief centrifugation at 10,000 x g, at 4°C, and washed three times with solubilization buffer. Proteins were eluted by re-suspending in two volumes of 2X SDS-sample buffer (10mM Tris, 15 mM SDS, 20 mM DTT, 20% glycerol,

0.02% bromphenol blue, pH 6.8) followed by incubation at 65°C for 30 minutes. Proteins were resolved by SDS-PAGE, transferred to Immobilon-P membranes (Millipore, Bedford, MA), and immunoblotted with anti-FLAG M2 (Sigma-Aldrich) primary antibodies and detected by anti-mouse AP-linked secondary antibodies (Bio-Rad) in Tris-buffered saline containing 5% powdered milk and 0.1% Tween-20, unless indicated otherwise.

### **In Vitro Translation**

Each construct was translated *in vitro* using the TnT Coupled Transcription/Translation System (Promega) following the company's protocol. This protocol simplifies *in vitro* translation by starting with cDNA. The addition of RNA polymerase to the translation mixture eliminated the separate synthesis of RNA from DNA. In brief, the TnT buffer, rabbit reticulocyte lysate, RNA polymerase, amino acid mixture, and RNase inhibitor were added to a 0.5 ml microcentrifuge tube placed on ice. 1 µg of plasmid DNA was added to the tube and briefly spun to mix reaction components to the bottom of tube. The reaction was then incubated at 30°C for 90 min.

### **Gel-overlay Assay**

Protein samples were separated by SDS-PAGE gel and transferred to Immobilon-P membranes (Millipore, Bedford, MA), incubated with *in vitro* translation product of FLAG-RPNI for 1 hr at room temperature. The membrane was washed for five minutes three times at room temperature with TTBS and immunoblotted with anti-FLAG primary antibodies (Sigma Aldrich). The association of the *in vitro* translated product was detected with anti-mouse AP-linked secondary antibodies (Bio-Rad) diluted in Tris-buffered saline containing 5% powdered milk and 0.1% Tween-20.

### **Construct siRNA of RPNI**

The GenScript's siRNA design center siRNA Target Finder and siRNA Construct Builder (<http://www.genscript.com/rnai.html>) was used to design siRNA sequence for RPNI with following nucleotide sequences:

*Sense1*:GATCCCGTTGTTCTCGTAATGTACTTTGTTGATATCCGCAAAG  
TACATTACGAGAACAATTTTTTCCAAA;*Antisense1*:AGCTTTTGGAAAA  
AATTGTTCTCGTAATGTACTTTGCGGATATCAACAAAGTACATTACG  
AGAACAACGG;*Sense2*:GATCCCATCTTCAGTGCATACTGGTCATTGAT  
ATCCGTGACCAGTATGCACTGAAGATTTTTTTCCAAA;*Antisense2*:AGC  
TTTTGGAAAAAAATCTTCAGTGCATACTGGTCACGGATATCAATGAC  
CAGTATGCACTGAAGATGG;*Sense3*:GATCCCGTATTGACAGTCTCATC  
AAAGTTTGATATCCGACTTTGATGAGACTGTCAATATTTTTTCCAAA;  
*Antisense3*:AGCTTTTGGAAAAAAATATTGACAGTCTCATCAAAGTCGGA  
TATCAAACCTTTGATGAGACTGTCAATACGG.

### **Confocal Microscopy**

Cells transfected with GFP-tagged vector, GFP-tagged RPNI, and GFP-tagged RPNI siRNA were grown in 6-well culture plates on glass coverslips to 60% - 75% confluency and fixed in 3.7% paraformaldehyde for 30 minutes. Adherent cells were treated with lysis buffer (0.1% Triton-X100, 150mM NaCl, 1mM EGTA, pH7.4) for 20 minutes. Then cells were incubated with mouse anti-HA antibody (1:1000) for 1 hour, followed by washing with PBS. Cells then were incubated with goat anti-mouse Alexa 594 (1:1000). All antibody incubations were performed in PBS with 10% BSA. Cells were dried briefly and mounted onto glass slides using Vectashield (Vector Labs, Burlingame, CA). HA-tagged

MOR was visualized by immunofluorescence, using BD CARVITM Confocal Imager with a Leica DMIRE2 fluorescence microscope.

### **Fluorescence Flow Cytometry**

Cells were grown in 12-well culture plates to 80%-85% confluency. Before the addition of antibodies, cells were rinsed twice with serum-free DMEM. Then the cells were incubated at 4 °C for 60 minutes in serum-free DMEM with anti-HA antibody (1:500). Afterward, the cells were washed twice with serum-free DMEM and incubated with Alexa633-labeled goat anti-mouse IgG secondary antibody (1:400) at 4 °C for 1 additional hour. Then the cells were washed and fixed with 3.7% formaldehyde before quantifying the receptor immunoreactivity with fluorescence flow cytometry (FACScan, BD Biosciences). Fluorescence intensity of 10,000 cells was collected for each sample. Cell Quest software (BD Biosciences) was used to calculate the mean fluorescence intensity of the cell population. In our study, two-color flow cytometry was used. A stained non-transfected sample (Mock) was processed with the cytometer to adjust the voltages on FSC and SSC detectors for viewing the populations of interest. The R1 region was adjusted around the population. The fluorescent detector voltages were adjusted to place the unstained events in the lower left quadrant. After that, each sample was installed and data were required. Only the cells that transfected with GFP were used to obtain the data on MOR fluorescence. All FACS analyses were conducted three times with triplicate samples in each experiment.

### **Results**

**Identification of RPNI direct binding to MOR.** In order to identify components of MOR signaling complexes, (His)<sub>6</sub>-MOR stably expressed in

N2A cells was partially purified with a Ni<sup>2+</sup> resin column and the proteins within the receptor complex were separated as described in Materials and Methods. Silver-staining of the gels revealed multiple protein bands including (His)<sub>6</sub>-MOR identified subsequently with western analysis, which migrated as a diffused band with molecular weight between 65-70 KDa (Fig S1A). Several protein bands were excised and analyzed using MALDI-TOF mass spectrometry as described. One of the proteins with significant mascot probability score (>65) was tentatively identified to be ribophorin I (RPNI). The protein band around 85 KD was demonstrated conclusively as being RPNI with the LC MS/MS spectrometry analysis. Five distinct peptides were identified from MS/MS spectra with >90% confidence (representing 9% sequence coverage) and 3 peptides were identified with <90% confidence. Total coverage (all peptides) was 13.6% by amino acid sequence (Table 1). Equivalent protein candidates reported were gi|74207369, gi|55715894, gi|48474583 and gi|31543605. They all refer to the sequence of RPNI. The distribution of the 5 peptides within the RPNI amino acid sequence was summarized in Figure 1A. To confirm whether MOR interacts with RPNI and whether this interaction occurs in intact cells, we carried out coimmunoprecipitation studies with lysate from N2A cells transiently transfected with MOR and RPNI. Expression of full length RPNI tagged at the N-terminus with the FLAG epitope was confirmed by direct Western analyses of the total lysates (Figure 1B, panel c). Interaction of RPNI with MOR was determined by coimmunoprecipitating the complex with antibodies against the HA epitope, followed by immunoblotting with anti-FLAG antibody. RPNI did not coimmunoprecipitate with the receptor when cells were transfected with either HA-MOR or FLAG-RPNI alone (Figure 1B, panel a, lane 1 and 2). However, RPNI was detected in anti-HA immunoprecipitates from cells that were co-transfected with both HA-MOR and

FLAG-RPNI, indicating that MOR interacts with FLAG-RPNI in mammalian cells (Fig. 1B, panel a, lane 3 and 4). Similarly, coimmunoprecipitation of HA-MOR with FLAG-RPNI was observed only in cells co-transfected with both HA-MOR and FLAG-RPNI using anti-FLAG, but not in cells transfected with either one of these two constructs (Figure 1B, panel b). Same results were also obtained when digitonin was used to extract the complex in order to preserve the oligosaccharidetransferase (OST) physiological activity (Fig S2B). Interestingly, although RPNI showed interaction with MOR in both Triton X-100 treated and digitonin treated immunoprecipitates, other components of OST complex only showed in digitonin treated immunoprecipitates (Fig S2B). Such observations could be due to fact that the four components of OST complex link to each other when OST stability was maintained in digitonin (Fu *et al.*, 1997) during co-IP of RPNI with MOR. RPNI interaction with MOR does not depend on the OST complex glycosylation activity. Only when the OST stability was maintained in digitonin, the individual components of OST complex were co-IP with MOR. Meanwhile, when the stability of OST complex was disrupted by Triton X-100, only RPNI but not RPNII, OST48, or Dad1 was co-immunoprecipitated with MOR (Fig S2).

The RPNI interaction with MOR can be demonstrated to occur within the cellular context, which is not a consequence of detergent extraction by the immunoprecipitation studies with the mixed lysates. When N2A cells separately transfected with MOR or RPNI were mixed together immediately prior to detergent addition for lysate preparations and co-IP, anti-HA did not co-immunoprecipitate FLAG-RPNI from mixed cells transfected with either MOR or RPNI while anti-HA could coimmunoprecipitate the FLAG-RPNI from N2A cotransfected with both MOR and RPNI (Fig 1C). The direct interaction between RPNI and MOR can be demonstrated further with gel-overlay

experiments as described in Materials and Methods. As shown in Figure 1D panel a, *in vitro* translation resulted in the production of the full-length FLAG-RPNI. After incubating the Immobilon-P membrane containing the SDS-PAGE separated total lysate from N2A cells with the *in vitro* translated products, positive interaction in the lane containing lysate from MOR-expressed N2A cells, but not in the lane from wild type N2A cells, was observed after excess *in vitro* translated product was removed by repeated washings (Figure 1D, panel b). The location of the *in vitro* translated FLAG-RPNI product coincided with the location of HA-MOR, as determined by immunoblotting with anti-HA antibody (Figure 1D, panel c). These data indicate that RPNI directly interacts with MOR, not via a protein scaffold or complex.

To demonstrate whether RPNI interacts with MOR endogenously expressed, MOR from mouse hippocampus tissue was immunoprecipitated by the anti-MOR C-tail polyclonal antibodies. Mouse cerebellum was used as the negative control to determine the specificity of the antibodies used. It showed that MOR C-tail antibodies could IP the endogenous RPNI from hippocampus but not from cerebellum extracts (Fig S3). In order to examine whether RPNI could associate with other glycosylated GPCRs, N2A cells were co-transfected with  $\alpha_{1A}$ -adrenergic receptor (AR1 $\alpha$ ) and RPNI transiently. Co-IP studies indicated that RPNI also interacted with AR1 $\alpha$  similar to the RPNI interaction with MOR, i.e., FLAG-RPNI was pulled down by anti-HA only in N2A cells expressing both FLAG-RPNI and HA-AR1 $\alpha$  (Fig S4A). Since RPNI is within the glycosyltransferase complex, the interaction between RPNI and MOR, between RPNI and AR1 $\alpha$  can occur within the endoplasmic reticulum (ER), prior to being transported to Golgi during the maturation of these GPCRs. The presence of MOR in ER or Golgi of N2A transiently transfected with MOR can

be observed with confocal microscopy studies using specific organelle markers. The co-localization of MOR and RPNI within the ER was observed in such confocal microscopy studies (Fig S5A).

**Ability of RPNI to affect cellular location of MOR.** To examine the effect of RPNI interaction on MOR cellular trafficking, three RPNI siRNA (#1,2,3) and one scramble siRNA were constructed as described in Materials and Methods. siRNA constructs were transfected into N2A cells and the GFP fluorescence was used to screen for similar transfection efficiency before lyses. The efficiency of RPNI siRNA knocking-down was demonstrated as Fig 2A. Only siRNA#3 construct exhibited significant knock down of the RPNI content in N2A cells. Thus, siRNA#3 and scramble siRNA as control were used in subsequent studies. N2A cells stably expressing HA-MOR were transfected with GFP-pRNAT H1.1/hygro vector (0.1 $\mu$ g), GFP-scramble RPNI siRNA (0.1 $\mu$ g) or GFP-RPNI siRNA#3 (0.1 $\mu$ g). MOR distribution was detected with mouse anti-HA antibody. We observed no difference in MOR distribution among cells transfected with scramble RPNI siRNA and the control vector. Comparing cells with no GFP fluorescence and those with, MOR was detected only on the cell surface in cells transfected with the scramble siRNA (Figure 2B). In N2A cells expressing the RPNI siRNA as indicated by the GFP fluorescence, the majority of MOR was detected to be located intracellularly (Figure 2C). In the same field, in cells not expressing the RPNI siRNA as indicated by the absence of GFP fluorescence, MOR was observed on the cell surface only. After siRNA transfection, total MOR expression was not altered as indicated by western analyses of the total lysate (Figure 2D). The cell surface MOR level with siRNA transfection was quantified with FACS using N2A cells transfected with GFP-Vector as the basal fluorescence level. The cell surface

receptor fluorescence decreased from  $100 \pm 5.4\%$  to  $41.96 \pm 2.9\%$  of the basal level after RPNI siRNA transfection (Figure 2D). These data demonstrate that RPNI regulates MOR cell surface expression. To eliminate the possibility that over-expression and knock-down of RPNI could affect the overall MOR glycosylation state leading to the removal of misfolded protein, the glycosylation states of MOR after over-expressing or knocking-down of RPNI were detected by western blot analyses following the treatment with Endoglycosidase H (EndoH) and PNGase F (EndoF). As summarized in Fig 3A panel a, majority of MOR migrated in SDS PAGE with a molecular weight  $\sim 65$ -70 KDa. There was a minor protein band with M.W.  $\sim 45$ -46 KDa detected by the HA antibodies, probably the immature form of MOR. Pretreatment of the lysate with EndoH reduced the M.W. of MOR slightly, while pretreatment with EndoF reduced the M.W. of MOR to  $\sim 46$  KDa, similar to that of the nascent polypeptide. Over-expression of RPNI eliminated the non-matured MOR protein band, but did not alter the receptor sensitivity toward EndoH and EndoF (Figure 3A, panel b). siRNA knockdown of RPNI resulted in an increase in the amount of immature MOR form, but did not alter the receptor sensitivity to these two enzymes (Figure 3A, panel c). Therefore, the observed cellular location of MOR under the conditions of over-expression of RPNI or knock-down of RPNI with siRNA does not reflect an alteration in the glycosylation states of the receptor.

Interestingly, interaction of RPNI with MOR appears to involve the glycosylation states of the receptor. As shown in Figure 3B, gel overlay studies with the *in vitro* translated RPNI product indicated that only MOR not treated with the enzymes could bind with RPNI. Pretreatment of MOR with either EndoH or EndoF eliminated the RPNI interaction with the receptor (Figure 3B, panel b). Since western analyses indicated similar level of receptor among

various enzyme treatments (Figure 3B, panel a), the absence of interaction in such gel overlay studies suggested the high mannose or some hybrid types of N-linked carbohydrates on MOR were essential for RPNI interaction. Combined with the data of RPNI IP from mixed cell lysates (Fig 1C), it indicates that carbohydrate (CHO) moiety is indispensable for RPNI binding. To further demonstrate whether RPNI interacts directly with the CHO moiety or not, the MOR partially purified with wheat germ agglutinin was digested with PNGase F and gel overlay studies were carried out with the *in vitro* translation product of RPNI. No interaction was observed between RPNI and MOR in the PNGase F treated sample (Fig 3B, panel b).

The inability of RPNI to interact with the PNGase F treated MOR could be due to the changes in the receptor's conformation after enzyme digestion thus affecting the recognition between these proteins, the role of CHO in RPNI binding was investigated with other GPCRs. Since our data showed RPNI could bind to glycosylated adrenergic receptor ( $\alpha_{1A}$  AR) (Fig S4A), whether RPNI could have distinct interaction among GPCRs that exhibit high sequence homology but different glycosylation states was investigated, such as the non-glycosylated  $\alpha_{2B}$ -AR and the highly glycosylated  $\alpha_{2C}$ -AR. As shown in Fig S4B and Fig S4C, RPNI was not co-IP with  $\alpha_{2B}$ -AR while RPNI did co-IP with  $\alpha_{2C}$ -AR. Despite the highly conserved motifs of them (Dong and Wu, 2006), our data suggested that there might not be specific binding motif for RPNI. N-glycosylation plays an important role in RPNI interaction with GPCR.

**RPNI enhances cell surface expression of the C2 mutant, but not the 5 N-glycosylation mutant.** Previous studies indicated that the export of MOR could

be facilitated by a chemical chaperone such as naloxone (Chaipatikul *et al.*, 2003). In particular, naloxone could rescue an export-deficient MOR mutant lacking a motif at the proximal carboxyl tail <sup>344</sup>KFCTR<sup>348</sup> (C2). Colocalization of C2 and MOR in ER has been reported (Chaipatikul *et al.*, 2003). The C2 mutant receptor had similar glycosylation state as the wild type receptor (Fig S6A), which gel-overlay studies indicated it could interact with RPNI directly (Fig 3C, panel a). Whether RPNI could increase the export of the C2 mutant was examined with confocal microscopy using anti-HA conjugated with Alexa<sup>488</sup> to detect the receptor location and goat anti-mouse antibody conjugated with Alexa<sup>594</sup> to detect the FLAG-RPNI. As shown in Fig 4A, cell surface expression of C2 mutant was observed only in N2A cells expressing both C2 mutant and RPNI. Meanwhile, in N2A cells without RPNI expression, i.e., cells exhibiting only the Alexa<sup>488</sup> fluorescence, majority of the C2 mutant was detected intracellularly (Fig 4A, panel b). RPNI and naloxone appear to have similar mechanisms in regulating C2 mutant expression. Using FACS analyses to determine the cell surface C2 level, we could demonstrate that the cell surface expression of C2 was dependent on the amount of RPNI plasmid used to transfect the cells. The addition of 1  $\mu$ M naloxone in cells expressing RPNI increased the amount of C2 on cell surface, but only at the lower RPNI plasmid concentration (Figure 4B). The level of C2 expressed on cell surface in the presence of naloxone and RPNI did not significantly exceed the level observed when naloxone alone was used to rescue the C2 export. The inability of naloxone to increase the cell surface expression of C2 in N2A cells over-expressed with RPNI could be the exhaustion of the intracellular located receptor export pools at the high level of RPNI. However, this did not appear to be the case since intracellular located C2 could be observed in N2A cells over-expressing RPNI (Figure 4A). These data suggest that RPNI may have

chaperone activities similar to that observed with the chemical chaperone naloxone.

Since RPNI was known to have oligosaccharyltransferase activity (Kelleher et al., 1992) and RPNI could not interact with MOR pretreated with EndoH or EndoF (Figure 3B), we investigated whether the putative glycosylation residues, Asn at the N-terminal domain of MOR, had roles in RPNI export function. The putative glycosylation sites in MOR (Asn<sup>9</sup>, Asn<sup>31</sup>, Asn<sup>38</sup>, Asn<sup>46</sup> and Asn<sup>53</sup>) were all mutated to Asp (MOR5ND). MOR5ND transiently transfected into N2A cells was observed to be retained at the ER (Fig S6B). Similar to the mobility of the PNGase F pretreated MOR, MOR5ND in SDS-PAGE exhibited an apparent MW of ~46KDa (Figure S6A). Also, gel-overlay studies indicated that MOR5ND, similar to MOR pretreated with EndoH or PNGase F, was unable to interact with RPNI (Figure 3C, panel a). When the cellular location of the receptor was monitored by confocal microscopy, MOR5ND was observed as intracellular location despite over-expression of RPNI (Figure 4C). Majority of the receptor immunofluorescence was detected intracellular in regardless of RPNI level (Figure 4C, panel b). Similarly, FACS analyses of the MOR5ND receptor mutant demonstrated minimal cell surface expression. Over-expression of RPNI resulted in slight, but not significant change in cell surface MOR5ND mutant receptor immunofluorescence. Interestingly, addition of naloxone did not result in an increase in cell surface expression of MOR5ND receptor mutant either, regardless of the presence or absence of RPNI over-expression (Fig 4D).

To determine whether chaperone function of RPNI is dependent on N-glycosylation, single mutation mutants in each of the 5 putative glycosylation Asn sites of MOR were generated. As shown in Fig S7B, all 5 single glycosylation site mutants exhibited a slightly faster mobility in SDS-PAGE,

indicative of a smaller molecular weight protein species than wild type MOR. In some regards, their molecular weights are similar to that of MOR pretreated with EndoH (Fig 3A). Interestingly, in contrast to the wild type MOR, all the single glycosylation site mutants could not pull down the FLAG-RPNI (Fig S7A). Hence, RPNI should have minimal consequence on these mutants' intracellular trafficking. When the cell surface expression of these mutants was determined by FACS analyses, it was shown that RPNI could not regulate the plasma membrane insertion of these mutants (Fig 5B). Although variable degrees of cell surface expression of the mutant receptors were observed (Fig 5A), co-expression of RPNI with any one of the five mutants did not increase these mutant receptors export to the cell surface. Such data suggest RPNI's interaction with MOR and subsequent chaperone function requires full N-glycosylation of the receptor.

**RPNI rescues C2 without increasing the mutant receptor interaction with calnexin.** The transit of proteins from ER is determined by its interaction with calnexin. Pharmacological chaperones were reported to rescue some GPCR mutants by altering their interaction with calnexin (Robert et al., 2005). It is probable that RPNI-enhanced cell surface expression of MOR is a reflection of the receptor interaction with calnexin. Hence, the export deficient mutant C2 was used to examine whether RPNI could increase C2 glycosylation level and subsequent calnexin binding. MOR and the C2 mutant were immunoprecipitated from N2A cells transfected either with HA-MOR and vector (Fig 6A, lane 1), with HA-C2 and RPNI (Fig 6A, lane 2), with HA-C2 and vector treated with naloxone (Fig 6A, lane 3), with HA-C2 and vector treated with the proteasome inhibitor MG132 (Fig 6A, lane 4), or with HA-C2 and vector treated with saline (Fig 6A, lane 5). The relative C2 receptor level

was determined using HA-MOR as the reference. The increase in the total cellular level of C2 in N2A cells over-expressed RPNI was similar to those observed in cells treated with naloxone or proteasome inhibitor MG132 (Fig 6B). However, FACS analysis showed that overexpression of RPNI, like addition of naloxone (Chaipatikul et al., 2003), increased the total C2 cell surface level while MG132 did not (Fig 6C). Also, in contrast to wild type MOR, in which strong interaction with calnexin was detected in the immunoprecipitate (Fig 6A lane 1 and Fig 6D), C2 did not exhibit strong interaction with calnexin (Fig 6A lane 2-5 and Fig 6D). Over-expression of RPNI or pretreatment with naloxone did not increase the receptor-calnexin interaction. These data suggest that the RPNI chaperone function, similar to that of naloxone, is not due to an increase in calnexin binding to MOR.

**RPNI interacts with DOR and KOR and enhances their export.** Since RPNI was shown to interact with other highly glycosylated GPCR such as AR1 $\alpha$  and  $\alpha$ 2C- but not  $\alpha$ 2B-AR (Figure S4), whether RPNI could interact with  $\delta$ -opioid receptor (DOR) or  $\kappa$ -opioid receptor (KOR) and had similar effect in these receptors' export was investigated. Coimmunoprecipitation studies were performed in lysate from N2A cells transiently transfected with HA-DOR or HA-KOR, together with either FLAG-RPNI or vector control. Similar to our observations with MOR, RPNI was observed to co-IP with DOR and KOR (Fig 7A and 7C). RPNI was not co-immunoprecipitated with anti-HA when N2A cells were not transfected with the HA-DOR or HA-KOR. FACS analyses indicated that RPNI also could affect DOR or KOR export. Overexpression of RPNI significantly increased the DOR level on the cell surface by  $33.2 \pm 7.8\%$  (Fig 7B), but did not significantly increase KOR cell

surface expression (Fig 7D). In comparison, when N2A cells were transfected with RPNI siRNA, both DOR and KOR cell surface expression were significantly reduced by  $38.1 \pm 3.9\%$  and  $22 \pm 4.4\%$ , respectively.

## Discussion

RPNI was originally identified as an integral component of rough microsomal membranes and appeared to be related to the bound ribosomes (Kreibich et al., 1978). Currently, RPNI is accepted to be a member of the oligosaccharyltransferase (OST) family. The mammalian OST is an oligomeric complex composed of three membrane proteins located within the ER: ribophorin I (RPNI), ribophorin II (RPNII) and OST48 (Kelleher et al., 1992). Later, DAD1, a anti-apoptotic protein, also was found to be a subunit of the mammalian OST (Kelleher and Gilmore, 1997). The biosynthesis of membrane proteins at the ER involves the integration of the polypeptide at the Sec61 translocon, together with a number of maturation events that can occur both during and after synthesis, such as N-glycosylation and signal sequence cleavage (Wilson et al., 2005). The transmembrane domain of RPNI has been suggested to function as a dolichol binding site (Kelleher et al., 1992). It is also reported that RPNI may function to retain potential substrates in close proximity to the catalytic subunit of the OST (sttp3), thereby stochastically improving the efficiency of the N-glycosylation reaction *in vivo* (Wilson et al., 2005). Other evidence has shown that RPNI may be multifunctional and facilitate additional processes, for example, ER quality control (Wilson et al., 2005).

Using an affinity column purification paradigm, we have identified RPNI as a MOR-interacting protein. The interaction between RPNI and MOR was confirmed by coimmunoprecipitation studies in transiently transfected N2A

cells and direct gel overlay studies using the *in vitro* translation products of a RPNI cDNA construct. By means of both confocal immunofluorescence microscopy and FACS analysis, our data demonstrated that the expression level of MOR could be regulated by RPNI level. RPNI appears to mediate MOR exocytotic activity, which is clearly related to its OST activity. For example, RPNI can stimulate the transport of the MOR C2 mutant from the ER to the cell surface, but not the export of the glycosylation-deficient MOR mutant-MOR5ND. This phenomenon suggests that RPNI not only is involved in biosynthesis of nascent polypeptides as previously reported, but also plays a pivotal role in their maturation and plasma membrane expression.

How RPNI can regulate MOR plasma membrane expression requires further investigation. However, our studies reveal several possible scenarios in which RPNI may affect MOR export.

First, our data showed that RPNI rescuing MOR C2 mutant was not due to ERAD (endoplasmic reticulum associated degradation) because ERAD substrate MOR could not rescue C2 (Law et al., 2005) and MG132 only enhanced intracellular accumulation of C2 mutant but not on cell surface, in contrary to RPNI overexpression (Fig 6C). Furthermore, over-expression of RPNI has differential effects on the export of various opioid receptors and MOR mutants (Fig 7&4).

Second, our data suggested that RPNI could serve as chaperone for MOR. RPNI has been suggested to be involved in ER quality control. (de Virgilio et al., 1998; Wilson et al., 2005). Antibodies produced against the cytoplasmic domain of RPNI interfere with protein translocation across the rough ER by preventing ribosome targeting to the Sec61 complex (Yu et al., 1990). OST was demonstrated to be adjacent to the protein translocation channel (Shibatani et al., 2005), allowing the cotranslational modification of the

nascent polypeptide as it enters the lumen of the rough ER (Chen et al., 1995). Most newly synthesized membrane and secretory proteins are delivered to the Sec61 translocon that mediates their integration into the lipid bilayer (Lecomte et al., 2003). The Sec61 translocon forms an aqueous pore that is gated by the luminal Hsp70—BiP (Alder and Johnson, 2004; Alder et al., 2005). Accumulating evidence has revealed that the ER molecular chaperone BiP is a master regulator of ER function. BiP is responsible for maintaining the permeability barrier of the ER during protein translocation, directing protein folding and assembly, and targeting misfolded proteins for retrograde translocation so they can be degraded by the proteasomes (Hendershot, 2004; Alder *et al.*, 2005). Hsp70 (BiP), together with RPNI, already has been found to interact with the ACE receptor (Santhamma and Sen, 2000). Interestingly, we identified one of the proteins co-purified with (His)<sub>6</sub>-MOR to be BiP. Thus, similar to the chemical chaperone of MOR—naloxone (Chaipatikul *et al.*, 2003), RPNI/Hsp70 could function as chaperone to rescue MOR C2 mutant transport to cell surface.

As the prelude of chaperone-assisted folding and oligomerization, formation of disulfide bonds already has started when the growing nascent peptide chains enter the luminal compartment (Bergman and Kuehl, 1979a, 1979b). Proteins that fail to fold or oligomerize properly are prevented from export and are degraded (Hurtley and Helenius, 1989; Doms, 1990; Parodi, 2000). During folding, polypeptides with N-linked oligosaccharides interact transiently and specifically with two ER-unique chaperones, calnexin and calreticulin. Calnexin transiently interacts with different glycoproteins during folding and maturation (Hebert et al., 1996). The disulfide bonds in the opioid receptor may link to calnexin and affect the plasma membrane expression of the opioid receptor. Interestingly, C2 mutant is different from some other calnexin-

retained GPCR mutants -V2 vasopressin receptor and V1b/V3 receptor mutants (Morello et al., 2001; Robert et al., 2005), which may account for different mutants having different effect on the interaction of calnexin. From Figure 6, calnexin was detected when MOR was immunoprecipitated, contrary to C2 coexpressed with RPNI. Coexpression of C2 and RPNI didn't affect the total amount of cellular glycosylated receptor, compared to C2 with naloxone and C2 with proteosome inhibitor MG132. Under all these conditions, interaction between C2 and calnexin was not detected (Fig 6D). However, the co-expression of RPNI with C2 helps to stabilize C2 and prevents its degradation, as compared to C2 co-transfected with vector control (Fig 6A&B). The data suggested that overexpression of RPNI could enhance cell surface expression of C2, which might reflect RPNI-associated ER quality control processes to facilitate C2 mutant's export out of ER other than the calnexin pathway.

The chaperone activity of RPNI appears to be connected to its OST activities. Contrary to the MOR C2 mutant, another MOR plasma membrane expression deficient mutant in which all 5 Asn residues at the N-terminus were mutated to Asp (MOR5ND), was unable to be expressed in plasma membrane despite RPNI over-expression. Furthermore, addition of naloxone did not result in cell surface expression of MOR5ND. On the other hand, one of the single Asn mutants, N53D, was shown to express on the cell surface (Fig 5) and interact with calnexin (Fig S8). Over-expression of RPNI or naloxone treatment did not increase the expression of the N53D mutant (Fig 5). These results suggest that N-glycosylation is critical for naloxone or RPNI to function as a chaperone. A new model for OST recently was proposed in which RPNI might act as a chaperone or as an escort to promote the N-glycosylation of selected substrates by the catalytic STT3 subunits (Wilson and High, 2007). The importance of N-glycosylation in opioid receptor plasma membrane expression

was demonstrated further with other opioid receptors—DOR and KOR, and the endoglycosidases studies. Although RPNI is known to form a complex with these two receptors, RPNI, as a chaperone, exhibits differential effects in their plasma membrane expressions. KOR has less N-glycosylation sites and over-expression of RPNI has minimal effect on KOR plasma membrane expression. However, by knocking-down RPNI level with siRNA, KOR plasma membrane expression decreased, illustrating that RPNI was important in KOR final destination. All these data suggest that RPNI's function depends not only on the glycosylation state of the receptor but also on the number of glycosylation sites.

Collectively, a major finding of this study is the interaction of MOR with RPNI in neuroblastoma cells and the potential function of this association in regulating opioid receptor plasma membrane expression. Our data indicate that RPNI has functions other than being an oligosaccharyltransferase. The interaction of RPNI with MOR suggests that RPNI serves as a chaperone or controller of MOR transport from the ER to the cell surface. It remains to be determined whether RPNI and its interaction with MOR can regulate or be regulated by receptor signaling.

*Acknowledgement:* We acknowledge the Center for Mass Spectrometry and Proteomics facility, BIPL, and Flow Cytometry Core Lab, University of Minnesota, for technical help. We also thank Dr Guangyu Wu for kindly providing us HA- $\alpha_{1A}$  AR, HA-AR2B and GFP-AR2C constructs.

## References

- Abeijon, C., and Hirschberg, C.B. (1992). Topography of glycosylation reactions in the endoplasmic reticulum. *Trends Biochem Sci* *17*, 32-36.
- Alder, N.N., and Johnson, A.E. (2004). Cotranslational membrane protein biogenesis at the endoplasmic reticulum. *J Biol Chem* *279*, 22787-22790.
- Alder, N.N., Shen, Y., Brodsky, J.L., Hendershot, L.M., and Johnson, A.E. (2005). The molecular mechanisms underlying BiP-mediated gating of the Sec61 translocon of the endoplasmic reticulum. *J Cell Biol* *168*, 389-399.
- Bergman, L.W., and Kuehl, W.M. (1979a). Co-translational modification of nascent immunoglobulin heavy and light chains. *J Supramol Struct* *11*, 9-24.
- Bergman, L.W., and Kuehl, W.M. (1979b). Formation of intermolecular disulfide bonds on nascent immunoglobulin polypeptides. *J Biol Chem* *254*, 5690-5694.
- Chaipatikul, V., Erickson-Herbrandson, L.J., Loh, H.H., and Law, P.Y. (2003a). Rescuing the traffic-deficient mutants of rat mu-opioid receptors with hydrophobic ligands. *Mol Pharmacol* *64*, 32-41.
- Chen, C., Li, J.G., Chen, Y., Huang, P., Wang, Y., and Liu-Chen, L.Y. (2006). GEC1 interacts with the kappa opioid receptor and enhances expression of the receptor. *J Biol Chem* *281*, 7983-7993.
- Chen, W., Helenius, J., Braakman, I., and Helenius, A. (1995). Cotranslational folding and calnexin binding during glycoprotein synthesis. *Proc Natl Acad Sci U S A* *92*, 6229-6233.
- Chen, Y., Mestek, A., Liu, J., Hurley, J.A., and Yu, L. (1993 Jul). Molecular cloning and functional expression of a mu-opioid receptor from rat brain. *Mol Pharmacol.*, *44*(41):48-12.
- de Virgilio, M., Weninger, H., and Ivessa, N.E. (1998). Ubiquitination is required for the retro-translocation of a short-lived luminal endoplasmic reticulum glycoprotein to the cytosol for degradation by the proteasome. *J Biol Chem* *273*, 9734-9743.
- Doms, R.W. (1990). Oligomerization and protein transport. *Methods Enzymol* *191*, 841-854.
- Dong, C., and Wu, G. (2006). Regulation of anterograde transport of alpha2-adrenergic receptors by the N termini at multiple intracellular compartments. *J Biol Chem* *281*, 38543-38554.

Evans, C.J., Keith, D.E., Jr., Morrison, H., Magendzo, K., and Edwards, R.H. (1992). Cloning of a delta opioid receptor by functional expression. *Science* 258, 1952-1955.

Fu, J., Ren, M., and Kreibich, G. (1997). Interactions among subunits of the oligosaccharyltransferase complex. *J Biol Chem* 272, 29687-29692.

Hebert, D.N., Foellmer, B., and Helenius, A. (1996). Calnexin and calreticulin promote folding, delay oligomerization and suppress degradation of influenza hemagglutinin in microsomes. *Embo J* 15, 2961-2968.

Helenius, A., and Aebi, M. (2001). Intracellular functions of N-linked glycans. *Science* 291, 2364-2369.

Hendershot, L.M. (2004). The ER function BiP is a master regulator of ER function. *Mt Sinai J Med* 71, 289-297.

Hurtley, S.M., and Helenius, A. (1989). Protein oligomerization in the endoplasmic reticulum. *Annu Rev Cell Biol* 5, 277-307.

Kapphahn, R.J., Ethen, C.M., Peters, E.A., Higgins, L., and Ferrington, D.A. (2003). Modified alpha A crystallin in the retina: altered expression and truncation with aging. *Biochemistry* 42, 15310-15325.

Kelleher, D.J., and Gilmore, R. (1997). DAD1, the defender against apoptotic cell death, is a subunit of the mammalian oligosaccharyltransferase. *Proc Natl Acad Sci U S A* 94, 4994-4999.

Kelleher, D.J., Kreibich, G., and Gilmore, R. (1992). Oligosaccharyltransferase activity is associated with a protein complex composed of ribophorins I and II and a 48 kd protein. *Cell* 69, 55-65.

Kieffer, B.L., Befort, K., Gaveriaux-Ruff, C., and Hirth, C.G. (1992). The delta-opioid receptor: isolation of a cDNA by expression cloning and pharmacological characterization. *Proc Natl Acad Sci U S A* 89, 12048-12052.

Kornfeld, R., and Kornfeld, S. (1985). Assembly of asparagine-linked oligosaccharides. *Annu Rev Biochem* 54, 631-664.

Kreibich, G., Freienstein, C.M., Pereyra, B.N., Ulrich, B.L., and Sabatini, D.D. (1978). Proteins of rough microsomal membranes related to ribosome binding. II. Cross-linking of bound ribosomes to specific membrane proteins exposed at the binding sites. *J Cell Biol* 77, 488-506.

Kreibich, G., Sabatini, D.D., and Adesnik, M. (1983). Biosynthesis of hepatocyte endoplasmic reticulum proteins. *Methods Enzymol* 96, 530-542.

Law, P.Y., Erickson-Herbrandson, L.J., Zha, Q.Q., Solberg, J., Chu, J., Sarre, A., and Loh, H.H. (2005). Heterodimerization of mu- and delta-opioid receptors occurs at the cell surface only and requires receptor-G protein interactions. *J Biol Chem* 280, 11152-11164.

Lecomte, F.J., Ismail, N., and High, S. (2003). Making membrane proteins at the mammalian endoplasmic reticulum. *Biochem Soc Trans* 31, 1248-1252.

Morello, J.P., Salahpour, A., Petaja-Repo, U.E., Laperriere, A., Lonergan, M., Arthus, M.F., Nabi, I.R., Bichet, D.G., and Bouvier, M. (2001). Association of calnexin with wild type and mutant AVPR2 that causes nephrogenic diabetes insipidus. *Biochemistry* 40, 6766-6775.

Parodi, A.J. (2000). Protein glucosylation and its role in protein folding. *Annu Rev Biochem* 69, 69-93.

Petaja-Repo, U.E., Hogue, M., Laperriere, A., Walker, P., and Bouvier, M. (2000). Export from the endoplasmic reticulum represents the limiting step in the maturation and cell surface expression of the human delta opioid receptor. *J Biol Chem* 275, 13727-13736.

Robert, J., Auzan, C., Ventura, M.A., and Clauser, E. (2005). Mechanisms of cell-surface rerouting of an endoplasmic reticulum-retained mutant of the vasopressin V1b/V3 receptor by a pharmacological chaperone. *J Biol Chem* 280, 42198-42206.

Santhamma, K.R., and Sen, I. (2000). Specific cellular proteins associate with angiotensin-converting enzyme and regulate its intracellular transport and cleavage-secretion. *J Biol Chem* 275, 23253-23258.

Shibatani, T., David, L.L., McCormack, A.L., Frueh, K., and Skach, W.R. (2005). Proteomic analysis of mammalian oligosaccharyltransferase reveals multiple subcomplexes that contain Sec61, TRAP, and two potential new subunits. *Biochemistry* 44, 5982-5992.

Shilov, I.V., Seymour, S.L., Patel, A.A., Loboda, A., Tang, W.H., Keating, S.P., Hunter, C.L., Nuwaysir, L.M., and Schaeffer, D.A. (2007). The Paragon Algorithm: A next generation search engine that uses sequence temperature values and feature probabilities to identify peptides from tandem mass spectra. *Mol Cell Proteomics*.

Silberstein, S., and Gilmore, R. (1996). Biochemistry, molecular biology, and genetics of the oligosaccharyltransferase. *Faseb J* 10, 849-858.

Wilson, C.M., and High, S. (2007). Ribophorin I acts as a substrate-specific facilitator of N-glycosylation. *J Cell Sci* 120, 648-657.

Wilson, C.M., Kraft, C., Duggan, C., Ismail, N., Crawshaw, S.G., and High, S. (2005). Ribophorin I associates with a subset of membrane proteins after their integration at the sec61 translocon. *J Biol Chem* *280*, 4195-4206.

Yu, Y.H., Sabatini, D.D., and Kreibich, G. (1990). Antiribophorin antibodies inhibit the targeting to the ER membrane of ribosomes containing nascent secretory polypeptides. *J Cell Biol* *111*, 1335-1342.

**Footnotes:**

This research was supported by the National Institutes of Health [Grants DA007339, DA016674, DA000564 and DA011806].

Address correspondence to: Xin Ge, Department of Pharmacology, University of Minnesota. 6-120 Jackson Hall, 321 Church St. SE, Minneapolis, MN 55455-0217, Email:gexx0019@umn.edu

## Legends for figures:

**Figure 1. Identification of RPNI as a MOR-associated protein.** (A) LC MS/MS analysis of the protein band corresponding to RPNI. The sequences in bold and underlined represent the RPNI amino acid sequences identified using tandem mass spectrometry after in-gel digestion of the protein-staining band. The protein sequence refers to gi|31543605. (B) Coimmunoprecipitation of FLAG-RPNI and HA-MOR. Panel a: FLAG-RPNI was detected after HA-MOR was immunoprecipitated (IP) from the cell lysate; panel b: HA-MOR was detected after FLAG-RPNI was immunoprecipitated from the cell lysates; panel c: the expression level of FLAG-RPNI was determined in 1/20 of the total lysate used in IP experiments; panel d: MOR was detected with rabbit polyclonal antibodies directed against the C-tail of MOR after HA-MOR was immunoprecipitated from the cell lysates. (C) Co-IP of FLAG-RPNI and HA-MOR in mixed cells that individually express FLAG-RPNI and HA-MOR. Lane 1: cells only express HA-MOR as negative control; lane 2: mixed cells that individually express FLAG-RPNI and HA-MOR; lane 3: cells that express both FLAG-RPNI and HA-MOR as positive control. (D) Gel-overlay of RPNI with MOR. Panel a: *in vitro* translation products of FLAG-RPNI, as indicated by Western analysis using anti-FLAG antibody; panel b: Gel-overlay of FLAG-RPNI on membranes containing SDS-PAGE separated N2A extract from cells expressing or not expressing HA-MOR; panel c: Western analysis of MOR expression.

**Figure 2. siRNA-mediated knockdown of RPNI decreased cell surface expression of MOR in N2A cells.** N2A cells were transfected with GFP-

tagged vector, GFP-tagged scramble RPNI siRNA or GFP-tagged RPNI siRNA for 48 hours. (A) Efficiency of siRNA used on knocking-down endogenous RPNI. siRNA #3 significantly reduced endogenous RPNI expression compared with others.  $\beta$ -actin was used as control and transfection efficiency was controlled as described in Results. (B) Transfection of cells with 0.1  $\mu$ g of scramble GFP-RPNI siRNA did not affect the expression of MOR on cell surface. (C) Transfection of 0.1  $\mu$ g GFP-RPNI siRNA decreased the expression of MOR on cell surface. In both (B) and (C), panel a: HA-MOR was stained by the mouse anti-HA monoclonal antibody and detected with the goat anti-mouse antibodies conjugated with Alexa 594; panel b: merge MOR with GFP-tagged RPNI scramble siRNA or GFP-tagged siRNA. Scale bar equals 10  $\mu$ . (D) Panel a: expression level of MOR in 1/20 fraction of each sample, which showed total MOR of each sample are almost the same; Panel b: FACS analyses of cell surface MOR expression in N2A cells transfected with RPNI siRNA as described in Materials and Methods. The bars represent the average  $\pm$  S.E.M. from three separated experiments carried out in triplicate. \*\* denotes  $p < 0.01$  when compared with cells transfected with vector.

**Figure 3. Glycosylation state of MOR when overexpressing or knocking down RPNI.** (A): Western-blot to detect MOR, MOR after EndoH digestion, and MOR after PNGase F digestion. panel (a): MOR in extract from N2A-MOR transfected with vector, after EndoH digestion, and after PNGase F digestion; panel (b): extract from N2A-MOR over-expressing RPNI, after EndoH digestion, and after PNGase F digestion ; panel (c): MOR in extract from N2A-MOR transfected with RPNI siRNA, MOR after EndoH digestion, and MOR after PNGase F digestion. (B): Gel-overlay of

RPNI with MOR, EndoH digested MOR, and PNGase F digested MOR. panel (a): Western-blot to detect N2A extract from cells expressing MOR, EndoH digested MOR, and PNGase F digested MOR. Panel (b): gel-overlay of *in vitro* translated FLAG-RPNI on membrane containing SDS-PAGE separated N2A extract from cells expressing MOR, EndoH digested MOR, and PNGase F digested MOR were carried out as described in Methods and Materials. (C) Gel-overlay of *in vitro* translated FLAG-RPNI with MOR C2 mutant or MOR5ND mutant. Panel a: Gel-overlay of FLAG-RPNI on membranes containing SDS-PAGE separated N2A extract from cells expressing MOR C2 mutant or MOR5ND mutant; panel b: Western analysis used to detect different glycosylated forms of MOR C2 and MOR5ND mutants using anti-MOR C tail polyclonal antibody.

**Figure 4. RPNI rescues C2 cell surface expression but not 5 N-glycosylation-site mutants of MOR.** (A) RPNI up-regulate the cell surface expression of export deficient MOR C2 mutant. Panels a: WT N2A cells were cotransfected with HA-MOR C2 mutant and FLAG-RPNI. C2 mutant expression was detected by rabbit anti-HA antibody conjugated with Alexa 488; panels b: merge of MOR C2 mutant and FLAG-RPNI that was determined by staining with mouse anti-FLAG monoclonal antibody and detected with goat anti-mouse antibodies conjugated with Alexa 594; Scale bar equals 10  $\mu$ . (B) FACS analyses of C2 cell surface expression in the presence of naloxone and over-expression of RPNI. N2A cells were transiently transfected with vector or 0.5  $\mu$ g RPNI or 1  $\mu$ g RPNI and MOR C2 mutant. The  and  bars represent averages  $\pm$  SEM of immunofluorescence in cells treated and not treated with 1  $\mu$ M naloxone after transfection in n=3 experiments. (C) RPNI failed to regulate the export

of 5 N-glycosylation-site mutants of MOR (MOR5ND). Panels a: WT N2A cells were cotransfected with (His)<sub>6</sub>-MOR5ND mutant and FLAG-RPNI. MOR5ND mutant expression was detected by rabbit anti-(His)<sub>6</sub> antibody conjugated with Alexa 488; panels b: merge of MOR5ND mutant and FLAG-RPNI that was determined by staining with mouse anti-FLAG monoclonal antibody and detected with goat anti-mouse antibodies conjugated with Alexa 594; Scale bar equals 10 μ. (D) Inability of RPNI or naloxone to rescue cell surface expression of MOR5ND as determined by FACS analyses. The bars represent the averages ± SEM of 3 separate experiments carried out in triplicate.

**Figure 5. Inability of RPNI to affect the export of 5 single N-glycosylation-site mutants.** (A) N2A cells were transiently transfected either with MOR mutant or MOR for 48 hours before cell surface receptor levels were determined by FACS analyses, as described in Materials and Methods. The bars represent the averages ± SEM of 3 separate experiments carried out in triplicate; (B) N2A cells were transiently transfected either with MOR mutant and vector, or MOR mutant and 1 μg RPNI for 48 hours before cell surface receptor levels were determined by FACS analyses, as described in Materials and Methods. The  and  and  bars represent the averages ± S.E.M. in 3 separated experiments carried out in triplicate in the absence and presence of RPNI overexpression or treatment with 1μM naloxone respectively, \*\* p denotes < 0.01 when compared with cells transfected with vector.

**Figure 6. RPNI did not increase C2 and calnexin interaction.** N2A cells were transfected either with HA-MOR and vector (panel A, lane 1), with

HA-C2 mutant and FLAG-RPNI (panel A, lane 2), with HA-C2 mutant and vector treated with naloxone (panel A, lane 3), with HA-C2 mutant and vector treated with 10  $\mu$ M MG132 16 hours prior to harvesting (panel A, lane 4), or with HA-C2 mutant and vector (panel A, lane 5). Immunoprecipitation and western analyses were carried out as described in *Materials and Methods*. (B) Relative intensities of C2 mutant levels using HA-MOR as a reference, and the amount of  $\beta$ -actin immunoactivities in each lane was used for loading control. The bars represent the average  $\pm$  SEM of 3 separate experiments. (C) FACS analyses of cell surface MOR C2 mutant after overexpression of RPNI, or the addition of MG132. (D) relative intensities of calnexin co-IP with HA-MOR using HA-MOR immunoreactivity as a reference, and  $\beta$ -actin immunoactivities in each lane were used for loading control. The bars represent the average  $\pm$  SEM of 3 separate experiments.

**Figure 7. Interaction between RPNI and DOR and KOR affects the receptors export.** (A) Co-IP of RPNI with DOR. N2A cells were transiently transfected either with vector and HA-DOR, vector and FLAG-RPNI, or FLAG-RPNI and HA-DOR, as described in Materials and Methods. Panel a: RPNI expression was detected with mouse anti-FLAG antibody in 1/20 total cell lysates; panel b: RPNI was detected with rabbit anti-FLAG after HA-DOR was immunoprecipitated from the cell lysates using mouse anti-HA antibodies; panel c: the amount of HA-DOR immunoprecipitated and loaded on each lane was demonstrated after stripping the blots used to detect RPNI. (B) Increase of DOR export by RPNI. N2A cells were transiently transfected either with HA-DOR and vector, HA-DOR and RPNI, or HA-DOR and RPNI siRNA for 48 hours before cell surface receptor levels were

determined by FACS analyses, as described in Materials and Methods. The bars represent the averages $\pm$ S.E.M. of n=3 experiments carried out in triplicate. \* p denotes < 0.05, \*\* p denotes < 0.01 when compared with cells transfected with vector. (C) Co-IP of RPNI with KOR. N2A cells were transfected either with vector and HA-KOR, vector and FLAG-RPNI, or FLAG-RPNI and HA-KOR, as described in Materials and Methods. Panel a: RPNI expression was detected with mouse anti-FLAG antibody in 1/20 total cell lysates; panel b: RPNI was detected with rabbit anti-FLAG after HA-KOR was immunoprecipitated from the cell lysates using mouse anti-HA antibodies; panel c: the amount of HA-KOR immunoprecipitated and loaded on each lane was demonstrated after stripping the blots used to detect RPNI. (D) Decrease in KOR export after RPNI knock-down. N2A cells were transiently transfected either with HA-KOR and vector, HA-KOR and FLAG- RPNI, or HA-KOR and RPNI siRNA for 48 hours before cell surface receptor levels were determined by FACS analyses, as described in Materials and Methods. The bars represent the averages $\pm$ S.E.M. of n=3 experiments carried out in triplicate. \* p denotes < 0.05 when compared with cells transfected with vector.

Table 1. Peptides identified using tandem mass spectrometry corresponding to mouse RPNI

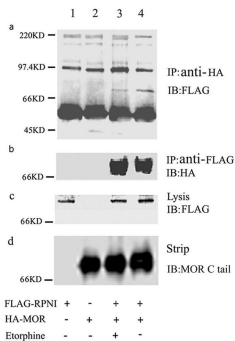
<i>Peptide</i>	<i>Confidence (%)</i>
AVTSEIAVLQSR	99
LPVALDPGSK	99
NIQVDSPLYDISR	99
SEDVLDYGPFK	97
DIPAYSQDTFK	91
DISTLNSGK	23
QPDSGISSIR	6
DTYLENEK	3

Confidence (%) as reported from Protein Pilot Results Summary. The percentage of total coverage is 13.6%. High confidence coverage (>90%) is 9%.

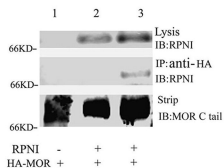
A

MESPVALLLL LLLCLGALAP TPGSASSEAP FLVNEDVKRT VDLSSHLAKV  
 TAEVVLVHPG GGSTRASSF VLALEPELES RLAHLGVQIK GEDEEDNNLE  
 VRETKIKGKS GRFFTVKLPV **ALDPGSKI**SV VVETVYTHVL HPYPTQITQS  
 EKQFVVFEGN HYFYSPYPTK TQTMRVKLAS RNVESYTKLG NPSR**SEDVLD**  
**YGFPKDIPAY** **SQDTFKVHYE** NNSPFLTITS MTRVIEVSHW GIIAVEENVD  
 LKHTGAVLKG PFSRYDQRQ PDSGISSIRS FKTILPAAQ DVYYRDEIGN  
 VSTSHLLILD DSVEMEIRPR FPLFGGWKTH YIVGYNLPSY EYLYNLGDGY  
 ALKMRFDVHV FDEQVIDSLT VKIILPEGAK **NIQVDSFYDI** SRAPDELHYT  
 YLDTFGRPVI VAYKKNLVEQ HIQDIVVHYT TNKVLMLQEP LLVVAIFYIL  
 FFTVIIYVRL DFSITKDPAA EARMKVACIT EQVLTLVNKR LGLYRHFDET  
 VNRYKQSRDI **STLNSGKSL** ETEHK**AVTSE** **I AVLQSR**LKT EGSDLCDRVS  
 EMQKLDQVK ELVLKSAVEA ERLVAGLKK DTYLENEKLS SGKRQELVTK  
 IDHILDAL

B



C



D

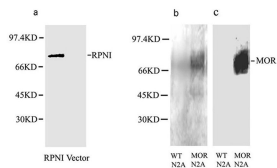


Fig 1

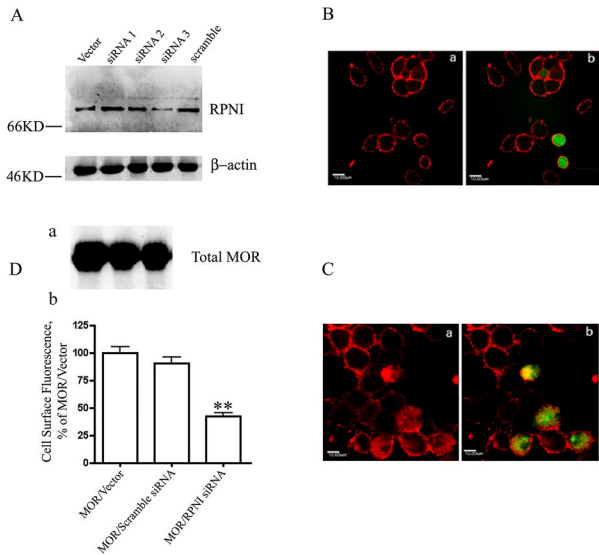


Fig 2

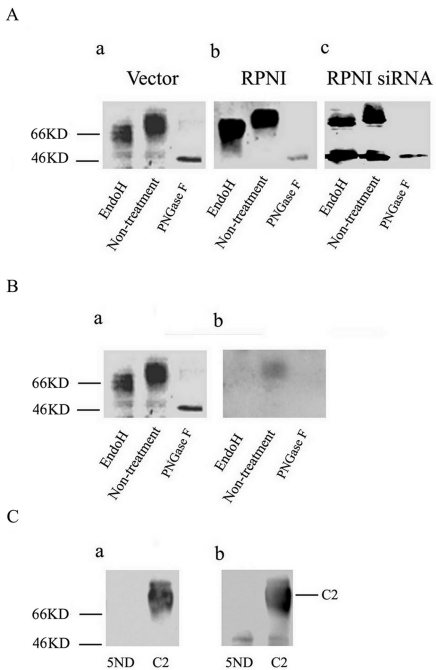
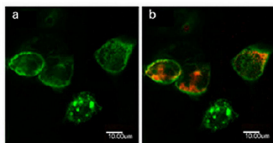
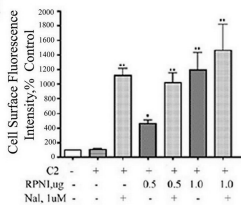


Fig 3

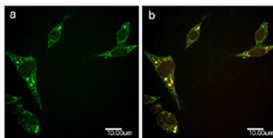
A



B



C



D

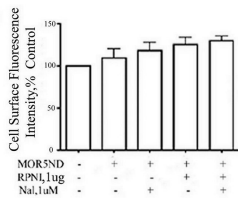
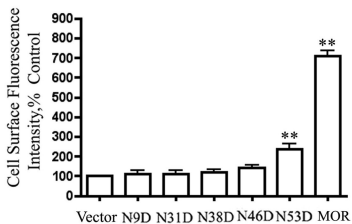


Fig 4

A



B

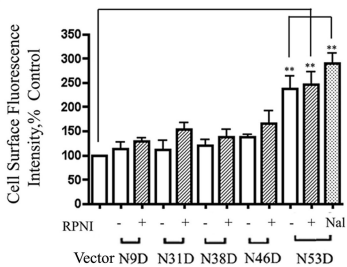
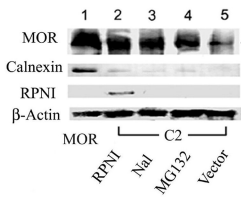
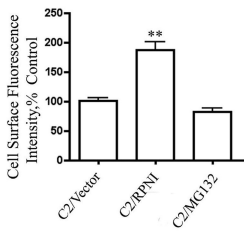


Fig 5

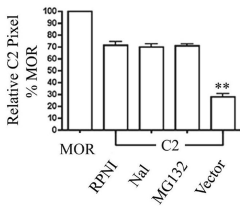
A



C



B



D

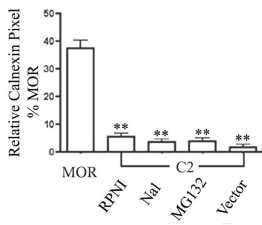


Fig 6

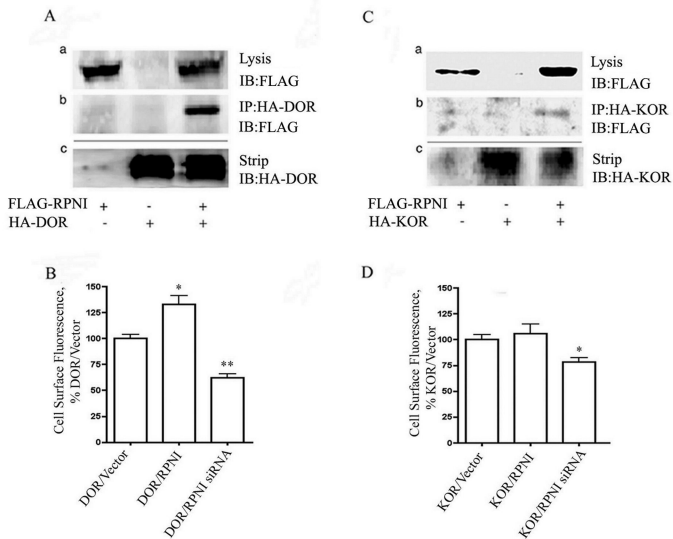


Fig 7